INFRARED THERMAL IMAGING ANALYSIS OF A 1-kW VARIABLE CAPACITY COMPRESSOR FREQUENCY INVERTER

Tiago de C. Macários
Jader R. Barbosa Jr.
POLO - Research Laboratories for Emerging Technologies in Cooling and Thermophysics, Department of Mechanical Engineering,
Federal University of Santa Catarina, Florianópolis, SC, 88040-900, Brazil
E-mail: jrb@polo.ufsc.br

Abstract. *The present paper deals with the experimental characterization via infrared thermography of the temperature distribution in the electronic components of a frequency inverter of a 1-kW cooling capacity variable speed refrigeration compressor. The transient thermal behavior was measured at the maximum compressor cooling capacity, and the tests were kept as closely as possible to real operating conditions by having the compressor connected to a hot-gas cycle calorimeter and the frequency inverter inside the hard plastic enclosure that protects the electronic components from airborne dust particles and moisture. The results reveal details about the thermal interaction between the components and the applicability of infrared thermography in the analysis of heat transfer effects inside closed cavities.*

Keywords: Infrared thermography, frequency inverter, electronics cooling, heat transfer.

1. INTRODUCTION

Recent advances in the fields of appliance manufacturing and electronics have enabled the development of variable capacity compressors (VCC) for refrigeration applications. When VCCs are used, the refrigerator cooling capacity can be changed continuously over a specific range in response to a change in the thermal load. In this way, by eliminating the need for successive on-off cycles, the refrigeration system as a whole consumes less energy — especially in times of low cooling load — and a better control of the temperature levels in the refrigerator compartments can be achieved.

In vapor compression refrigeration systems equipped with positive displacement compressors, the cooling capacity is given by:

$$Q = \frac{V_d f \Delta h_e}{v} \tag{1}$$

where v is the refrigerant specific volume at the compressor suction chamber, V_d is the swept volume, f is the compressor operating frequency and Δh_e is the specific refrigerating effect, i.e., the difference between the specific enthalpies of the refrigerant at the evaporator outlet and inlet.

In Eq. (1), the swept volume is a geometric parameter, the enthalpy variation is a function of the system evaporating pressure and the refrigerant specific volume is defined by the compressor geometry and its operating conditions. Therefore, the only parameter that can be easily changed to render a variable cooling capacity is the operating frequency.

Frequency inverters perform a three-stage electric energy conversion to deliver a variable frequency output to the compressor electric motor. The first stage consists of a diode bridge, which is responsible for converting alternating current (ac) into direct current (dc). The second stage comprises a filter that rectifies the dc signal to a continuous level. An arrangement of insulated-gate bipolar transistors (IGBTs) is the principal part of the third stage. IGBTs are fast switching components that let the previous rectified wave pass proportionally to the electric tension at which they are ionized. If the IGBTs are ionized at correct periods, a new harmonic wave characterized by a different frequency from the input will be generated.

Effective heat dissipation and temperature control are key issues in the design of electronic equipment as they are directly related to the system reliability (Garimella *et al.*, 2008). The majority of electronic components that comprise frequency inverters and other electronic equipment are strongly affected by the operating temperature. For example, the diode current has an exponential relation with temperature. The component gain of transistors is also strongly related to temperature. Capacitors are rated according to the maximum capacitance change over a certain temperature range. Inductors have a similar behavior. For resistors, a linear dependence exists between resistance and temperature.

Infrared (IR) thermal imaging (thermography) has long been acknowledged as a very effective means of providing accurate and reliable temperature data of electronic circuits and microprocessors (Linnander, 1993; Hamann *et al.*, 2007; Cheng *et al.*, 2008). Non-intrusiveness is the greatest upside of IR thermography. Since the temperature sensor does not need to be in contact with the surface being measured, there are no thermal inertia effects. Electronic components normally have small sizes and the mass of a thermocouple can interfere with the measurement. The spatial resolution of IR thermal imaging is no match for intrusive techniques, as detailed temperature maps can be produced instantaneously on a single

frame. On the other hand, the major downside of IR thermography is the difficulty to assess and calibrate radiation heat transfer parameters, such as the reflected environment temperature, the surface emissivity and the transmissivity. Thus, temperature measurements via IR thermography usually have much larger uncertainties than calibrated thermocouples, and the surrounding environment conditions play a much more important role in the measurement.

Linnander (1993) discussed basic issues related to the infrared wavelength, object size and temperature compensation during the temperature measurement of electronics components on PCBs. He also presented guidelines for determining emissivities of different components. Meinders *et al.* (1997) utilized thermal imaging to evaluate the local convective heat transfer coefficient associated with the heat transfer from copper cubes covered by epoxy resin used to simulate the components of a PCB. Cheng *et al.* (2008) combined infrared thermography measurements with a finite element method to determine the heat transfer characteristics of printed circuit boards taking into account the effect of thermal balls and thermal vias. Brito Filho and Henriquez (2010) developed a method to identify zones of high current concentrations that consisted of infrared thermography measurements. The method was tested in a microwave device (duplexer).

Recently, infrared thermography has been used to characterize the spatially resolved temperature distribution in dual core microprocessors. In order to gain visual access to the microprocessor, while maintaining the operating temperatures within safe limits, the metal heat sinks were replaced by a combination of infrared semi-transparent media, such as sapphire and mineral oil that cools the surface of the chip by forced convection (Hamann *et al.*, 2007; Mesa-Martínez *et al.*, 2007; Farkhani and Mohammadi, 2010; Ardestani *et al.*, 2010). This experimental method can be used as a validation tool for modeling techniques and for determining temperature-performance and power-performance efficiencies of alternate execution modes (Hamann *et al.*, 2007).

The purpose of this paper is to characterize the thermal profile of the electronic components on the PCB of a frequency inverter of a 1-kW variable cooling capacity compressor (VCC). The temperatures were measured with IR thermography and the operating conditions of the compressor were kept as closely as possible to the real application by having it running in a hot-gas cycle calorimeter built specifically for this study. The PCB was maintained inside its original hard plastic enclosure that serves the purpose of insulating the electronic components from dust particles and moisture in the ambient air. As a result, heat rejection from the components to the external environment occurs chiefly via an aluminum finned heat sink that is in thermal contact with the PCB and is located on one side of the enclosure. Additionally, a fraction of the heat generated in the enclosure is transferred to the ambient air by an association of natural convection (inside and outside the enclosure) and conduction (plastic cover) resistances on the remaining sides of the plastic box. Since the plastic cover is not transparent to infrared radiation, holes had to be drilled in order to gain visual access to the electronic components. To avoid disrupting the natural circulation pattern inside the inverter enclosure, the holes were covered with a plastic adhesive tape whose transmissivity to the infrared radiation was also determined as part of this work. The emissivities of the surfaces of the electronic components were determined and calibrated using standard procedures set forth by the infrared camera manufacturer.

The temperatures of the electronic components were measured via infrared imaging under transient (compressor start-up) and steady state conditions for the maximum compressor cooling capacity. The results were compared with those obtained with thermocouples, for some components, with a satisfactory level of agreement (i.e., within the experimental uncertainties associated with each technique).

2. EXPERIMENTAL WORK

2.1 Test apparatus

The test apparatus consisted of a hot-gas cycle calorimeter (see Fig. 1) in which the 1-kW compressor was installed. For a given amount of gas in the system (refrigerant charge), the calorimeter enabled the control of the suction and discharge pressures by means of hand-operated valves located at the compressor suction and discharge lines. A tube-fin heat exchanger was used for rejecting the compressor power as heat to the ambient. In the pressure enthalpy diagram, the idealized processes 1-2, 2-3 and 3-1 correspond to the compression, heat transfer in the heat exchanger and pressure drop in the valves, respectively. The working fluid was R-404A. The compressor speed was controlled by the frequency inverter that, in turn, was operated by means of a computer program supplied by its manufacturer. The power dissipated in the inverter was displayed by the software interface.

2.2 Frequency inverter

The frequency inverter used in this work is shown schematically in Fig. 2. The lower side (opposite to the one shown in Fig. 2) of the PCB could not be put directly in contact with the aluminum heat sink because each component was at a different electrical potential and the heat sink itself was an electrical conductor. Therefore, a gap filler had to be placed between the PCB and the heat sink. As the material from which the gap filler was made restricted the current leakage from the components, it also created a thermal resistance between the components and the external environment.

Figure 3 presents the footprint of the circuit board, where the shaded central region represents the area where the

(a) 'Hot'-gas cycle calorimeter.
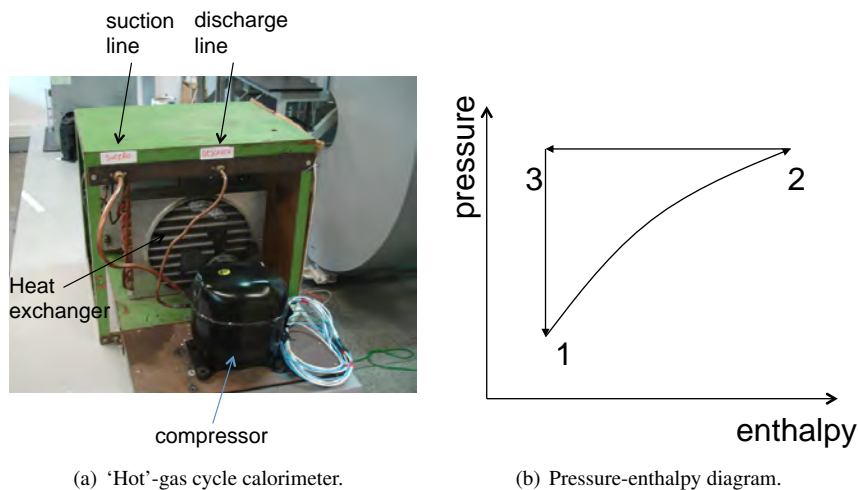
(b) Pressure-enthalpy diagram.
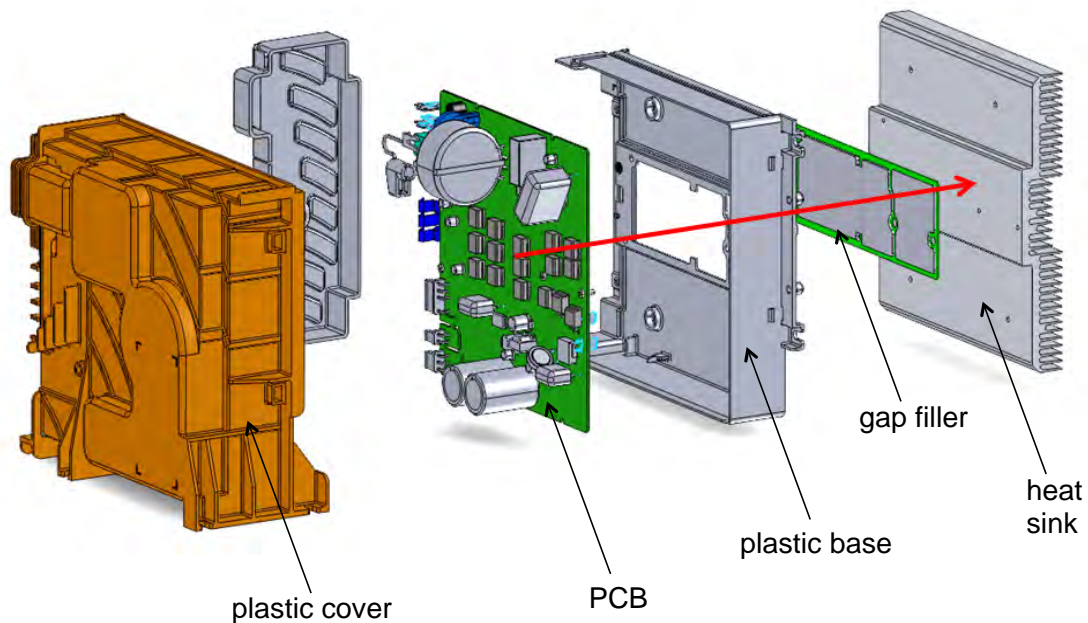
Figure 1. Compressor test apparatus.

Figure 2. Exploded view of the heat sink and the main heat transfer path from the PCB to the heat sink.

components had a heat conduction path to the external heat sink via the gap filler. Table 1 shows the rates of heat generation in each component, according to the inverter manufacturer. As mentioned before, since the board was kept inside a plastic enclosure, the thermal resistance imposed by the heat sink path had a major impact on the temperature of the components.

Natural convection takes place inside the plastic enclosure. The heat transfer coefficients associated with this mode of heat transfer are generally small, so the power dissipated per unit surface area in each component (see Table 1) can serve as an indication of which components will be hotter. The estimated surface temperature was the main selection criterion for identifying the components to be evaluated via infrared thermography. Therefore, all of the components in the heat sink region were chosen for the measurements, apart from diodes D301 and D302, because they were located in a region of difficult visual access. Also, the inductors and capacitors were chosen due to the different nature of their surfaces, as will be explained later.
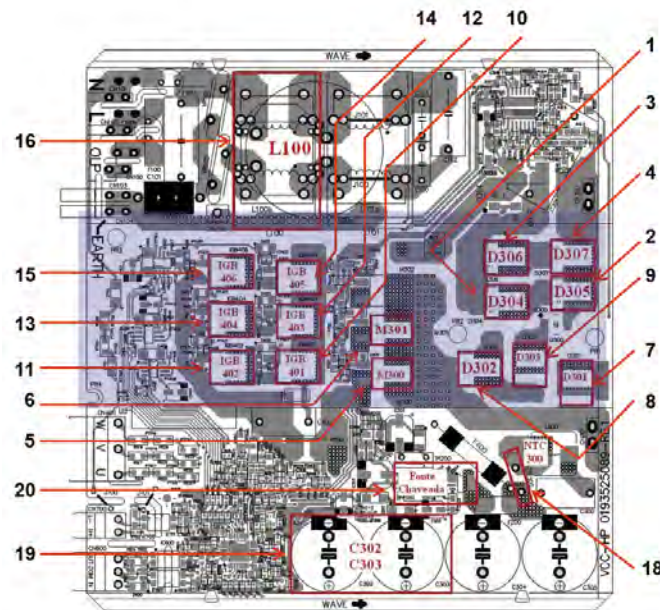
Figure 3. Frequency inverter PCB footprint. The shaded area in the center of the picture represents the approximate position of the gap filler, which thermally connects the PCB to the heat sink.

Table 1. Summary of the characteristics of the heat exchanger prototypes.

Component No.	Component Name	Power (W)	Heat flux (W/cm^2)
1	Rectifier Diode (D304)	2.1	0.455
2	Rectifier Diode (D305)	2.1	0.455
3	Rectifier Diode (D306)	2.1	0.455
4	Rectifier Diode (D307)	2.1	0.455
5	Mosfet Boost (M300)	4.6	0.996
6	Mosfet Boost (M301)	4.6	0.996
7	Diode Boost (D301)	3.7	0.801
8	Diode Snubber (D302)	1.8	0.390
9	Diode Snubber (D303)	1.8	0.390
10	IGBT (IGB401)	3.5	0.758
11	IGBT (IGB402)	3.5	0.758
12	IGBT (IGB403)	3.5	0.758
13	IGBT (IGB404)	3.5	0.758
14	IGBT (IGB405)	3.5	0.758
15	IGBT (IGB406)	3.5	0.758
16[+]	EMI Inductor (L100)	3.4	0.050
17[*,+]	Boost Inductor (Attached to enclosure)	7.6	N.A.
18[+]	NTC (300)	1.7	N.A.
19[+]	Capacitor (C302 & C303)	0.7	0.010
20[+]	Switched-mode power supply	2.0	0.192
	Total	61.3	

[*]The boost inductor is not seen in Fig. 3 because it is not mechanically connected to the PCB. Rather, it is attached to the plastic cover at approximately the same position as the rectifier diodes.
[+]Component not thermally connected to the heat sink.

2.3 Experimental procedure

2.3.1 Determination of the plastic tape transmissivity

As mentioned before, natural convection was the heat transfer mode inside the plastic enclosure. A hole-saw was used to create openings on the plastic enclosure that allowed visual access to the electronic components. The holes were

covered with a single layer of ordinary adhesive tape so as not to disrupt the air circulation pattern inside the cavity.

As the adhesive tape attenuates the infrared radiation, a temperature correction is needed. The procedure for determining the tape transmissivity consisted of heating a test surface to roughly 20 K above room temperature. With the test surface temperature measured independently by a surface thermocouple, the adhesive tape was placed between the measurement surface and the camera. As the temperature measured by the camera changed, the transmissivity was adjusted in the camera software to match the original temperature. The transmissivity determination apparatus consisted of a benchtop electric heater for setting the desired temperature on the test surface. The test surface itself was a metallic plate whose surface was covered with a material of known emissivity (black vinyl insulating tape). The transmissivity of the adhesive tape was estimated as 0.92.

2.3.2 Determination of surface emissivity of the electronic components

The surface emissivity is one of the most important parameters associated with infrared imaging techniques (Minkina and Dudzik, 2009). In the present work, due to the large number of electronic components with distinct surface characteristics, a careful procedure (based on manufacturer guidelines) was adopted to determine the surface emissivities of the electronic components on the PCB.

The procedure consisted of placing a piece of insulating tape (emissivity of 0.97) on the surface of the electronic component. Then, the component was heated to at least 20 K above the ambient temperature. A thermal image that contained a covered and an uncovered region was captured and, due the proximity between them and low thermal resistance of the tape (small thickness), their temperatures should be approximately the same. Thus, the emissivity of the uncovered region could be determined by changing its value in the camera software until the temperatures of both regions became equal. A similar procedure was used to determine the reflected temperature, according to the camera manufacturer.

2.3.3 Experimental tests

The experimental measurements were carried out at the maximum compressor power (approximately 1 kW). In this way, a thermal profile in the frequency inverter PCB was generated for the most critical operating condition.

During the experiments, the ambient temperature was not as stable as desired, since another experiment was being conducted in the same room and both experiments required high power. Thus, the temperature oscillated between 22°C to 26°C. Such perturbations are believed not to have affected the thermal performance since most thermal resistances were quite high. All tests were conducted over a transient period in which the compressor was switched on, and the components' temperatures increased from the room temperature up to their final values at steady state.

3. EXPERIMENTAL RESULTS

3.1 Validation against thermocouple measurements

Figure 4 shows a comparison of temperature measurements of selected components by means of infrared thermography and calibrated type-T thermocouples attached to the surfaces of the components. Very good agreement (within the experimental uncertainties of the techniques) is observed at later times when the temperature increase is exponential with time and after that, when steady state is approached.

Nevertheless, at earlier times (ten minutes or less into the test), the temperatures measured via infrared thermography are consistently higher than those given by the thermocouples, possibly as a result of the thermal inertia associated with the latter. This effect was more apparent for the components with a faster temperature change rate (MOSFET 301 and IGBT 403), for which temperature differences between infrared thermography and thermocouples were as high as 15°C before the first minute.

3.2 IGBTs and MOSFETs

The IGBTs (insulated gate bipolar transistors) and MOSFETs (metal oxide semiconductor field effect transistors) correspond to components 10-15 (IGBTs) and 5-6 (MOSFETs) in Fig. 3 and Table 1. They are the components with the highest rates of heat dissipation in the frequency inverter. Figure 5(a) shows a photograph of the components on the PCB through the hole on the plastic cover of the inverter. As mentioned previously, a small piece of insulating tape was placed on the upper right corner of each component to serve as a control surface for the determination of the surface emissivity. Figure 5(b) presents an infrared snapshot of the steady-state operation of the IGBTs and MOSFETs, with the control regions (i.e., those covered with insulating tape) shown as a white square. The actual surface of the component is identified with a black square. Due to the characteristics of the surfaces of the IGBTs and MOSFETs, it was concluded from the experimental analysis that their emissivities are very close to that of the insulating tape (0.97).

Figure 6 illustrates the thermal response of the IGBTs and MOSFETs. The particular run shown in this figure is one in which the system was switched off for about ten minutes. Despite the temperature differences between the components, it
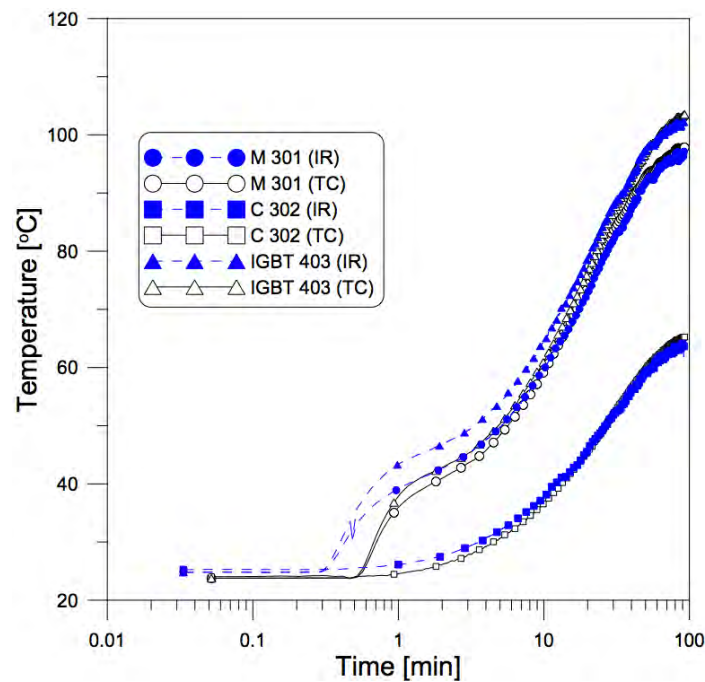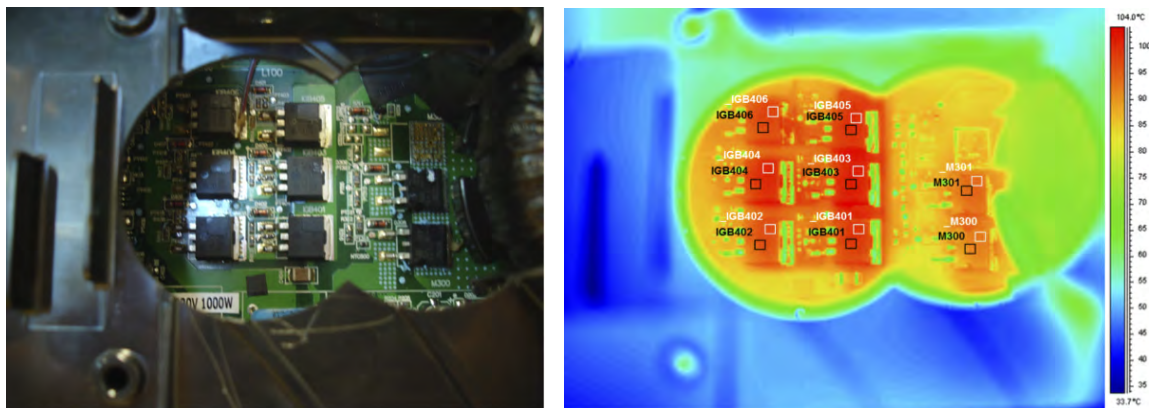
Figure 4. Comparison of infrared thermography and thermocouples for some selected components.

(a) Photograph of the components.

(b) Steady-state thermal image.

Figure 5. IGBTs and MOSFETs.

can be inferred that the time constants for the IGBTs and MOSFETs are practically the same, as their transient behavior was similar and they took approximately the same time to reach steady state once the compressor was switched on again. Nevertheless, some trends can be perceived in the temperature profiles shown in Fig. 6, which may be associated with the position of the components on the board. Firstly, the temperatures of IGBTs 401, 403 and 405 are consistently higher than those of the other IGBTs (402, 404 and 406). It is hypothesized that this is because IGBTs 401, 403 and 405 are in the thermal wake of C302 and C303 and are closer to MOSFETs 300 and 301 (which dissipate large quantities of heat). Hence, they are surrounded by warmer air than IGBTs 402, 404 and 406.

3.3 Overall thermal behavior of the PCB components

Figure 7 shows the temperature behavior of several inverter components during the course of a test at full compressor speed (maximum cooling capacity). As expected, the components located in the central region (IGBTs, MOSFETs and rectifier diodes) are those with the highest temperatures due to their highest heat dissipation rates.

The capacitors, which exhibited the lowest thermal profile among all components, have a much larger surface area compared to IGBTs and MOSFETs. They also have different materials covering their top (aluminum) and side surfaces (plastic wrapping), as can be seen from Fig. 8, which shows the temperature profile of C303. Due to their internal layered structure, heat transfer was assumed anisotropic and the largest heat dissipation rate was assumed to be through the top (flat) surface of the components.
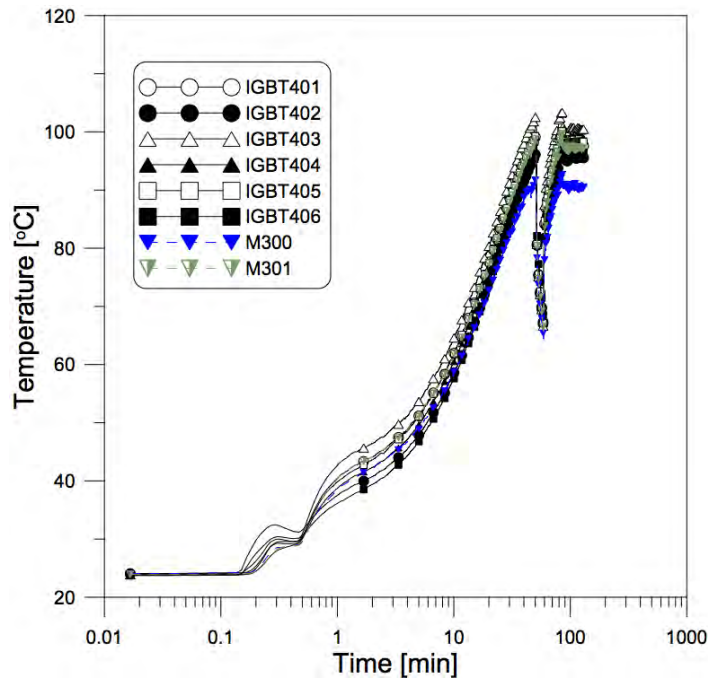
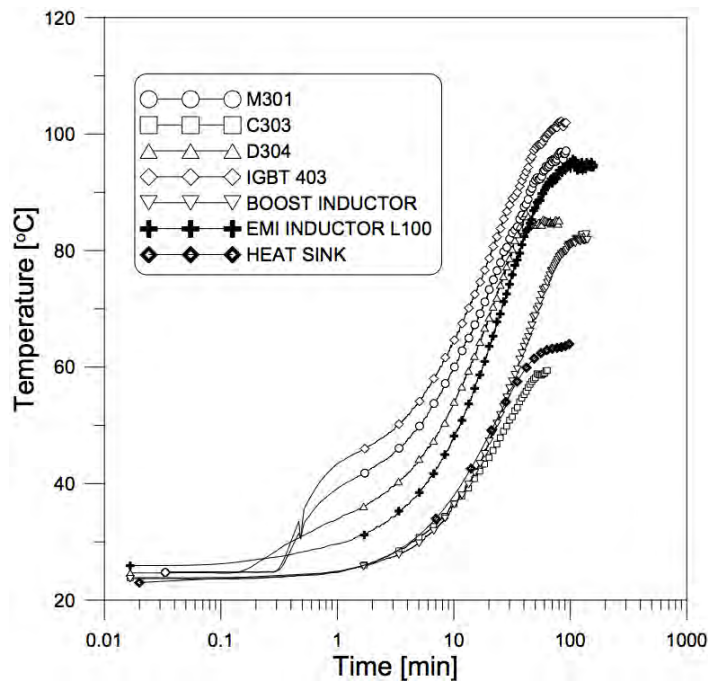Figure 6. Temperature behavior of the IGBTs and MOSFETs.

Figure 7. Temperature behavior of several types of components.

Initially, the same procedure of the IGBTs and the MOSFETs was used to measure these components temperatures (Fig. 8), but the reflection on the aluminum seals made it impossible to determine their emissivity. To circumvent this problem, the seals were fully covered with the electrical tape.

The temperature measurements on the capacitors with the insulating tape on the top surface agreed to within $\pm$ 3°C with thermocouple measurements at steady state (Fig. 4). As expected (and verified in Fig. 7), the temperatures of the capacitors are significantly smaller than those of the IGBTs and MOSFETs because of the lower heat dissipation rate and larger surface area, as can be verified from Table 1.

The external casing of the rectifier diodes (D304, D305, D306 and D307) are generally made from the same material (epoxy resin) as the IGBTs and MOSFETs, so the same value of emissivity has been set for these components. Also, an experimental procedure identical to that for the IGBTs and MOSFETs was adopted. The diodes' temperature measurement was presented with a peculiar situation because the infrared camera could not be positioned perpendicularly to the plane
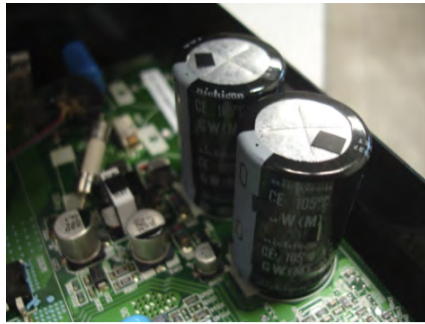
Figure 8. Capacitors C302 and C303 with a small piece of insulating tape on the aluminum (top) surface. Temperatures were acquired via infrared thermography with the top surface fully covered by the tape.

of the PCB, as was the case with the other components. This was because the opening on the plastic cover had to be cut on its side wall (the one to which the arrow "plastic cover" is pointing in Fig. 2). As a result, it was not possible to adjust the camera focus to all rectifier diodes at the same time. From some tests made during dummy runs, the errors arising from the lack of a proper focus on the components generated errors between 1 and 2°C, which are within the experimental uncertainties expected for the techniques involved. Figure 7 shows the temperature profile of D304, whose behavior was closely followed by the other rectifier diodes.

The characterization of the temperature of the inductors (Boost Inductor and EMI Inductor L100) was initially a challenge because of the difficulty associated with the calibration of the surface emissivity. The issue was that the temperatures measured on the control region (covered by the insulating tape) were always lower than the actual inductor surface temperature. So, in order to match temperatures, the surface emissivity would have to be set as greater than unity. Two possible explanations were sought for the problem. The first one was that, since the surface of the inductor was not flat, the tape was not at the same temperature as the inductor windings. The second explanation was that the surface of the inductor caused excessive reflection, which rendered the measurements unreliable. Covering the inductors surfaces with an opaque paint of known emissivity solved the problem (see Fig. 9). Figure 9(b) shows the infrared thermal map at steady state. As can be seen, the whole component reaches almost the same temperature despite of its large size. This is caused mainly because of the confined space where it is assembled.
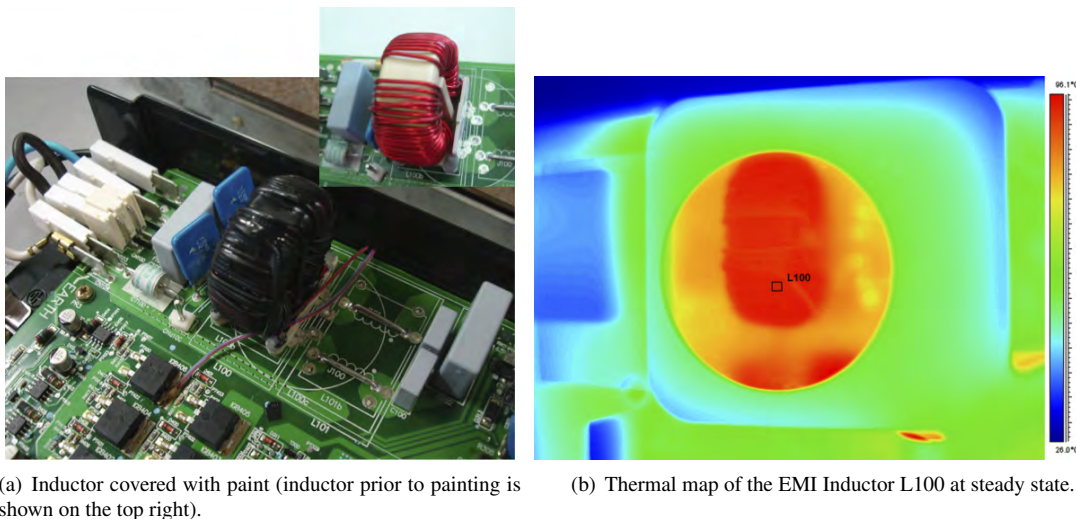

(a) Inductor covered with paint (inductor prior to painting is shown on the top right).

(b) Thermal map of the EMI Inductor L100 at steady state.

Figure 9. Analysis of the EMI Inductor L100.

As can be seen from Fig. 7, the EMI Inductor L100 exhibits a steeper temperature change rate and reaches an equilibrium temperature that is higher than that of the boost inductor, despite the fact that the heat dissipation rate of the latter is higher. This behavior may be linked to the fact that the core of the EMI Inductor L100 was made from plastic, while that of the other inductor was made from a metal alloy. Also, the positioning of EMI Inductor L100 in the thermal wake of the IGBTs (the hottest components on the board) certainly has contributed to its relatively higher temperature.

In order to generate thermal images for the extruded aluminum heat sink, its surface also had to be coated with black paint (Fig. 10). Also, electrically insulating tape tape was placed at some specific points of the surface to validate the emissivity settings. The infrared image of the heat sink, seen in Fig. 10(b), shows a small but significant gradient on the mid plane of the heat sink, which means that part of the heat is being conducted in the plane of the heat sink.
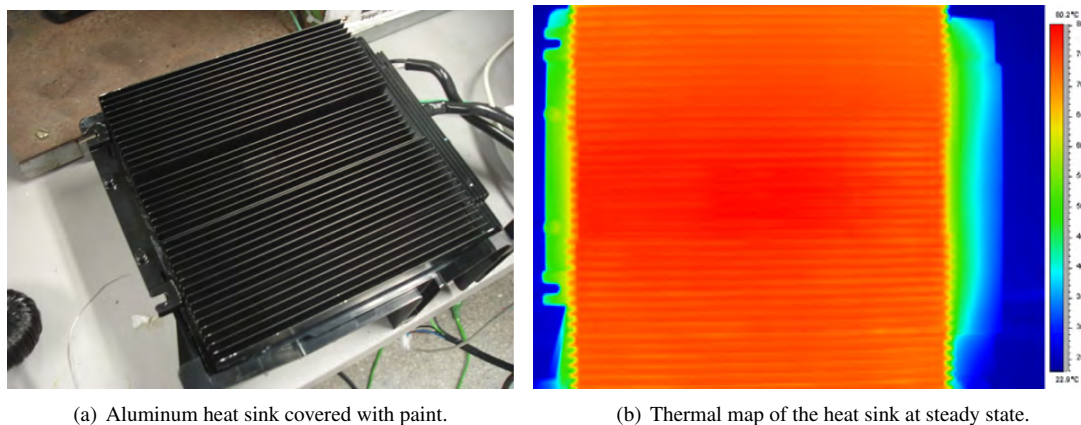
(a) Aluminum heat sink covered with paint.

(b) Thermal map of the heat sink at steady state.

Figure 10. Analysis of the aluminum heat sink.

4. CONCLUSIONS

The temperature distribution in the electronic components of the frequency inverter of a 1-kW variable cooling capacity compressor was investigated in the present study. The temperatures were measured with infrared thermography at real compressor operating conditions. The inverter was maintained inside its original hard plastic enclosure, so that the real operating conditions of the inverter were also respected.

In order to avoid disrupting the natural convection flow field inside the inverter cavity, the openings cut on the plastic cover were sealed with an adhesive tape whose infrared transmissivity was determined experimentally.

The IGBTs exhibited the largest and fastest temperature variation among all components, while capacitors C302 and C303 were those with the smallest temperature change. At steady state, the infrared thermography measurements agreed to within $\pm\ 3°C$ with calibrated type-T thermocouples.

Infrared thermography helped to understand the effect of the position of the components on their thermal behavior. For instance, the temperatures of IGBTs 401, 403 and 405 were higher than those of IGBTs 402, 404 and 406 because the former are surrounder by warmer air than the latter due to their proximity to MOSFETs 300 and 301 and to capacitors C302 and C303.

5. ACKNOWLEDGEMENTS

6. REFERENCES

Ardestani, E.K., Mesa-Martínez, F.J. and Renau, J., 2010. "Cooling solutions for processor infrared thermography". In *Proc. 26th IEEE SEMI-THERM Symposium*. Santa Clara, CA, pp. 187–190.

Brito Filho, J.P. and Henriquez, J.R., 2010. "Infrared thermography applied for high-level current density identification over planar microwave circuit sectors". *Infrared Physics & Technology*, Vol. 53, pp. 84–88.

Cheng, H.C., Chen, W.H. and Cheng, H.F., 2008. "Theoretical and experimental characterization of heat dissipation in a board-level microelectronic component". *Applied Thermal Engineering*, Vol. 28, pp. 575ÃŘ–588.

Farkhani, F.F. and Mohammadi, F.A., 2010. "Temperature and power measurement of modern dual core processor by infrared thermography". In *Proc. 2010 IEEE International Symposium on Circuits and Systems (ISCAS)*. Paris, France, pp. 1603–1606.

Garimella, S.V., Fleisher, A.S., Murthy, J.Y., Keshavarzi, A., Prasher, R., Patel, C., Bhavnani, S., Venkatasubramanian, R., Mahajan, R., Joshi, Y., Sammakia, B., Myers, B.A., Chorosinski, L., Baelmans, M., Sathyamurthy, P. and Raad, P., 2008. "Thermal challenges in next-generation electronic systems". *IEEE Transactions on Components and Packaging Technologies*, Vol. 31, pp. 801–815.

Hamann, H.F., Weger, A., Lacey, J.A., Hu, Z., Bose, P., Cohen, E. and Wakil, J., 2007. "Hotspot-limited microprocessors: Direct temperature and power distribution measurements". *IEEE Journal of Solid-State Circuits*, Vol. 42, pp. 56–65.

Linnander, B., 1993. "When it's too hot to touch use infrared thermography". *Circuits and Devices*, Vol. July, pp. 35–37.

Meinders, E.R., van der Meer, T.H., Hanjalic, K. and Lasance, C.J.M., 1997. "Application of infrared thermography to the evaluation of local convective heat transfer on arrays of cubical protrusions". *International Journal of Heat and*

Fluid Flow, Vol. 18, pp. 152–159.

Mesa-Martínez, F.J., Nayfach-Battilana, J. and Renau, J., 2007. "Power model validation through thermal measurements". In *Proc. of the 34th Annual International Symposium on Computer Architecture ISCAS07*. San Diego, CA, pp. 302–311.

Minkina, W. and Dudzik, S., 2009. *Infrared Thermography: Errors and Uncertainties*. Springer.

7. RESPONSIBILITY NOTICE

The authors are the only responsible for the printed material included in this paper.